Optimal Deployment of Energy Harvesters with Anti-Correlated Energy Generation at Base Stations

Doris Benda*, Sumei Sun†, Xiaoli Chu*, Tony Q.S. Quek‡ and Alastair Buckley*
* University of Sheffield, United Kingdom
† Institute for Infocomm Research, A*STAR, Singapore
‡ Singapore University of Technology and Design, Singapore
E-mail: dcbenda1@sheffield.ac.uk, sunsm@i2r.a-star.edu.sg, x.chu@sheffield.ac.uk,
tonyquek@sutd.edu.sg, alastair.buckley@sheffield.ac.uk

***Abstract*—Due to the intermittency of renewable energy generation, base stations (BSs) powered by renewable energy harvesters will experience power surpluses and power deficits over time. To use the renewable power more efficiently, energy harvesters with anti-correlated energy generation profiles should be deployed at BSs that are connected by transmission lines and power should be transmitted from surplus BSs to deficit BSs via transmission lines. In this paper, we develop an optimization algorithm to determine how energy harvesters with anti-correlated energy generation profiles should be deployed to every BS by taking into account the topology of the cellular network, i.e., whether or not a transmission line exists between a pair of BSs. Therefore, a BS is deployed more likely with an energy harvester type that is anti-correlated to those deployed at its connected neighboring BSs with our proposed algorithm. In addition, our proposed algorithm takes into account the distance-dependent power loss in the transmission lines. As a result, the shorter the transmission line between a pair of BSs, the more likely that these two BSs are deployed with anti-correlated energy harvesters. The renewable power that can be transmitted from the surplus BSs to the deficit BSs in the cellular network is on average around 40% higher with our proposed optimization algorithm in comparison with randomly deploying anti-correlated energy harvesters to the BSs.**

***Index Terms*—Cellular network, energy generation diversification, energy harvesting, energy sharing, renewable energy**

I. Introduction

Data traffic in cellular networks is growing exponentially [1]. As a result, network densification is necessary [1]. The more base stations (BSs) are deployed in a cellular network, the more energy is consumed by the cellular network. To alleviate the negative impact on the environment and on operators' energy bills, renewable energy-harvesting BSs are proposed for future cellular networks [2], [3].

BSs powered by renewable energy face the problem of temporal variations in the energy supply. These variations have to be managed properly to make efficient use of the harvested renewable energy. Energy generation diversification can mitigate the temporal variations in the energy supply at the BS by combining energy sources with anti-correlated energy generation profiles. Thus, the energy deficit in one profile can be compensated by an energy surplus of another profile. For instance, 80% of energy was saved in [4] between a pair of energy-sharing BSs with anti-correlated sinusoidal energy profiles. The benefits of energy generation diversification have been comprehensively studied in smart grids and conventional power grids [5]–[7]. Energy generation diversification in cellular networks powered by renewable energy sources has been mainly studied by combining wind energy and solar energy [2], [3]. The anti-correlation between solar and wind energy generation profiles is justified on a daily timescale by the fact that high pressure (low pressure) areas tend to be sunny (cloudy) with low (high) surface wind, and on a seasonal timescale by the fact that solar (wind) energy is higher in summer (winter) than in winter (summer) for many locations [2].

It is especially promising to connect nearby BSs with power transmission lines [8]–[10] and to deploy energy harvesters with anti-correlated energy generation profiles at BSs that are connected by power transmission lines. As a result, power can be transmitted from surplus BSs to deficit BSs via the transmission lines.

II. Proof of Concept

To demonstrate the concept of energy harvesters with anti-correlated energy generation profiles, we use a southeast orientated photovoltaic (PV) cell (energy harvester type 0) and a southwest orientated PV cell (energy harvester type 1) in London in June as an example. Southeast, and southwest orientated PV cells have an orientation angle of $-45°$, and $45°$ with respect to the southern direction, respectively (cf. Fig. 1). The effects of different PV cell orientation angles on the energy generation profiles are comprehensively studied in [11]–[13]. While energy harvester type 0 has a high power generation during time step 1 (potential surplus), energy harvester type 1 suffers from a low power generation (potential deficit), as seen in Fig. 2. Vice versa in time step 2, while energy harvester type 0 has a low power generation (potential deficit), energy harvester type 1 has a high power generation (potential surplus). Each BS is deployed with one of the two energy harvester types and all BSs have the same constant

energy consumption profile for simplicity in this example, as seen in Fig. 2. To make efficient use of the renewable power, power should be transmitted via transmission lines from BSs equipped with energy harvester type 0 to BSs equipped with energy harvester type 1 in time step 1. Vice versa in time step 2, power should be transmitted via transmission lines from BSs equipped with energy harvester type 1 to BSs equipped with energy harvester type 0.

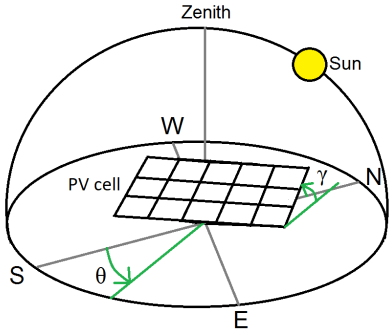

Fig. 1: Depiction of a PV cell installed with the orientation angle θ and with the inclination angle γ.

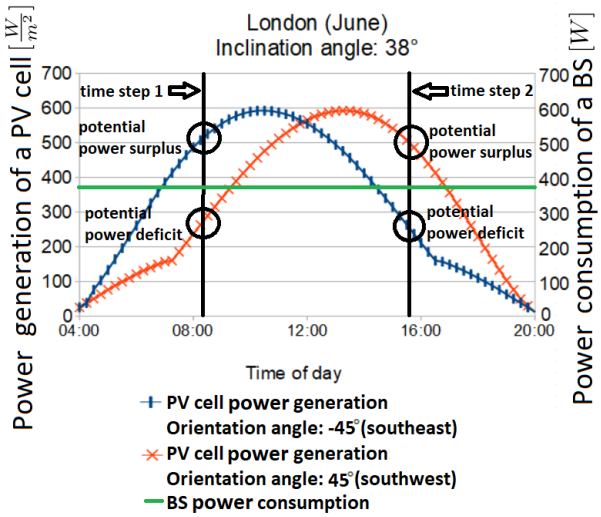

Fig. 2: A southeast orientated PV cell and a southwest orientated PV cell in London in June are used to demonstrate the concept of energy harvesters with anti-correlated energy generation profiles. The historical average time series data of the PV cells were derived from [14].

III. Contributions

The main contributions of this paper can be summarized as follows:

- We develop an optimization algorithm that can be run once during the cellular network planning to determine how energy harvesters with anti-correlated energy generation profiles should be deployed to every BS.
- We take into account the topology of the cellular network as well as the distance-dependent power loss in the transmission lines during the optimization.
- The optimization objective is to maximize the power that can be transmitted from surplus BSs to deficit BSs in the cellular network.
- We compare our proposed optimization algorithm with randomly deploying anti-correlated energy harvesters to the BSs. We investigate the effects of different numbers of BSs, different transmission line existence probabilities, different transmission line power loss coefficients, and different power surplus values.

IV. System Model

We consider $N \in \mathbb{N}$ uniformly distributed BSs in a square area of l^2 square meters, which are denoted by BS_i, $i \in \{1, ..., N\}$, $l \in \mathbb{N}$ (cf. Fig. 3). The parameter $c_i \in \{0, 1\}$ denotes if the BS_i is equipped with the energy harvesting device type 0 or the energy harvesting device type 1, e.g., either with a solar cell or a wind turbine. A BS_i with energy harvesting device type 0, i.e., $c_i = 0$, belongs to cluster 0 and is depicted with a black node in Fig. 4. A BS_i with energy harvesting device type 1, i.e., $c_i = 1$, belongs to cluster 1 and is depicted with a red node in Fig. 4.

The BS clustering optimization algorithm will be run once during the cellular network planning to determine for every BS its cluster and the corresponding energy harvesting device type.

The difference between the power generation and consumption of BS_i is denoted by the power surplus/deficit value $p_i^t[W]$ in watts for time step $t \in \{1, 2\}$. A surplus in power, and a deficit in power at BS_i are indicated by a positive value p_i^t, and a negative value p_i^t, respectively. The power surplus/deficit values of BSs in the same cluster at a given time step are similar because they are equipped with the same energy harvesting device type and have a similar BS load, hence we assume that all BSs in the same cluster have the same power surplus/deficit value at a given time step.

The energy generation profile of BSs in cluster 0 is anti-correlated to the energy generation profile of BSs in cluster 1. In other words, BSs of cluster 0, and cluster 1 have a power surplus of $b_0 \in \mathbb{R}^+$, and a power deficit of $b_1 \in \mathbb{R}^-$ in time step 1, respectively. Vice versa in time step 2, BSs of cluster 0, and cluster 1 have a power deficit of b_1, and a power surplus of b_0, respectively. The power surplus/deficit values p_i^t[1] are summarized as follows:

[1]We assume that every BS has a similar total daily energy consumption. Therefore, the energy harvesting device types should have similar capacities. The capacity of an energy harvesting device should not be oversized or undersized for powering one BS, that means we can assume that every BS will experience power surpluses and power deficits throughout the day. The time during a day where energy harvesting device 0 produces more power than the energy harvesting device 1 is represented by time step 1, whereas the time during a day where energy harvesting device 1 produces more power than the energy harvesting device 0 is represented by time step 2. Hence, it is justified to use only two time steps $t \in \{1, 2\}$ in our system model to represent the whole day. Because our optimization is done only once in a BS's lifetime, p_i^t represents the average daily power surplus/deficit value at the BS throughout the whole lifetime of the BS. Thus, we can assume that throughout the whole lifetimes of the BSs, the power surplus/deficit values at the BSs in the same cluster at a given time step are the same because they are equipped with the same energy harvesting device type and have a similar BS load. Because the energy harvesting device types have similar capacities, we can assume that $p_0^1 = p_1^2 = b_0$ and $p_1^1 = p_0^2 = b_1$.

$$p_i^t = \begin{cases} b_0 & c_i = 0 \text{ and } t = 1 \\ b_1 & c_i = 1 \text{ and } t = 1 \\ b_1 & c_i = 0 \text{ and } t = 2 \\ b_0 & c_i = 1 \text{ and } t = 2. \end{cases} \quad (1)$$

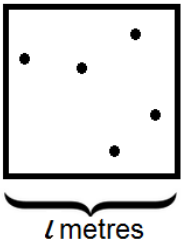

Fig. 3: Illustration of the considered cellular network with $N = 5$ BSs uniformly distributed in a square area of l^2 square meters.

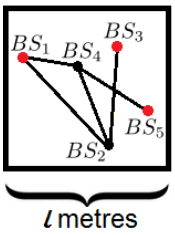

i	c_i	p_i^1	p_i^2
1	1	b_1	b_0
2	0	b_0	b_1
3	1	b_1	b_0
4	0	b_0	b_1
5	1	b_1	b_0

Fig. 4: The graph representation of the cellular network with example BS cluster allocation values c_i, surplus/deficit power values p_i^1 in time step 1 and surplus/deficit power values p_i^2 in time step 2 given for the BSs.

The normalized Euclidean distance $d\big((i,j)\big)$ between BS_i and BS_j with respect to l meters is as follows:

$$d\big((i,j)\big) = \frac{||BS_i - BS_j||}{l}, \quad (2)$$

where $||BS_i - BS_j||[\mathrm{m}]$ in meters is the Euclidean distance between BS_i and BS_j, and $l[m]$ in meters is the side length of the square in Fig. 4.

Power can be transmitted from a surplus BS in one cluster to a deficit BS in the other cluster at each time step if the two BSs are connected by a transmission line. The power flow in the transmission line is subject to power loss due to resistive heating. The power loss $P_{\text{loss}}\big((i,j)\big)[\mathrm{W}]$ in watts in the transmission line from BS_i to BS_j can be calculated by Ohm's law and the formula for the transmission line resistance [15] as follows:

$$P_{\text{loss}}\big((i,j)\big) = I^2 \cdot \rho \cdot \frac{l \cdot d\big((i,j)\big)}{A_{\text{c}}} = I^2 \cdot C \cdot d\big((i,j)\big), \quad (3)$$

where $I[\mathrm{A}]$ in amperes is the electric current traveling through the transmission line, $\rho[\Omega\mathrm{m}]$ in ohm-meters is the resistivity of the transmission line, $l[\mathrm{m}]$ in meters is the side length of the square in Fig. 4, $d\big((i,j)\big)$ is defined in (2), $A_{\text{c}}[\mathrm{m}^2]$ in square meters is the cross-sectional area of the transmission line, and $C[\Omega]$ in ohms is the power loss coefficient per l meters of transmission line, i.e., $C = \frac{\rho \cdot l}{A_{\text{c}}}$.

The topology of the cellular network is represented by a graph (cf. Fig. 4), where V is the set of vertices which denotes the BSs, and E is the set of directed edges which denotes the transmission lines as follows:

$$\begin{aligned} V =& \{1, 2, ..., N\}, \\ E =& \{(i,j), (j,i) | i \in V, j \in V, BS_i \text{ and } BS_j \text{ are} \\ & \text{connected by a transmission line}\}, \end{aligned} \quad (4)$$

where (i,j) denotes the directed edge from BS_i to BS_j.

The power flow on the edge (i,j) is denoted by $f^t\big((i,j)\big)$ in time step $t \in \{1,2\}$.

We justify the following two assumptions in our system model.

- We justify that the power flow is equivalent to the second power of the electric current flow in the transmission line in this paragraph. The electric power P in the transmission line can be calculated as follows:
$$P = V \cdot I, \quad (5)$$
where V is the electric potential, and I is the electric current. The power loss $P_{\text{loss}}\big((i,j)\big)$ in the transmission line is caused by the electric current and not the electric potential of the power as seen in (3). Nonetheless, it is outside of the scope of this paper to model the relationship between the power flow and the electric current flow in the transmission line. Hence, we assume for simplicity and in accordance with (5) that if the power increases/decreases in the transmission line, the electric current and the electric potential increase/decrease equally. In other words, a power flow in the transmission line of x watts is equivalent to a flow of $I = \sqrt{x}$ amperes and $V = \sqrt{x}$ voltages in our system model. Hence, the parameter $f^t\big((i,j)\big)[W/A^2]$ can be interpreted as the power flow on the edge (i,j) in watts or the second power of the current flow I^2 on the edge (i,j) in square amperes.
- We justify that $C \in \big[0, \frac{1}{\sqrt{2}}\big]$ in this paragraph. The maximum normalized distance $d\big((i,j)\big)$ in a square is $\sqrt{2}$. If C were greater than $\frac{1}{\sqrt{2}}$, then $C \cdot d\big((i,j)\big)$ could be greater than 1. That would imply that more power is lost in the transmission line than was sent through the transmission line.

We normalize all power values with respect to the constant value of $\max\{b_0, |b_1|\}$ as follows:

$$\begin{aligned} \hat{f}^t\big((i,j)\big) &= \frac{f^t\big((i,j)\big)}{\max\{b_0, |b_1|\}} \\ \hat{b}_0 &= \frac{b_0}{\max\{b_0, |b_1|\}} \\ \hat{b}_1 &= \frac{b_1}{\max\{b_0, |b_1|\}}. \end{aligned} \quad (6)$$

V. Mixed-Integer Linear Programming Problem

The objective is to find the optimal BS cluster allocation values c_n for all $BS_n, n \in V$, i.e., deploying either an energy harvesting device type 0 or an energy harvesting device type 1 at every BS, so that the renewable power in the cellular network can be used most efficiently. c_n, $\hat{f}^1\big((i,j)\big)$ and $\hat{f}^2\big((i,j)\big)$ are the parameters to be determined for all $n \in V$ and $(i,j) \in E$. Because the parameters c_n are integers whereas the power flow values $\hat{f}^t\big((i,j)\big)$ are real numbers, we need a mixed-integer linear programming solver for this problem.

The optimization objective is to maximize the total normalized renewable power M received at the deficit BSs during the two time steps as follows:

$$M = \max_{\mathbf{c},\hat{\mathbf{f}}^{\mathbf{1}},\hat{\mathbf{f}}^{\mathbf{2}}} \Big\{ \underbrace{\sum_{(i,j)\in E} \hat{f}^1\big((i,j)\big)\big(1 - C \cdot d\big((i,j)\big)\big)}_{\text{time step 1}} + \underbrace{\sum_{(i,j)\in E} \hat{f}^2\big((i,j)\big)\big(1 - C \cdot d\big((i,j)\big)\big)}_{\text{time step 2}} \Big\} \tag{7}$$

subject to

Lower bounds and upper bounds for the parameters to be determined:

$$\begin{aligned} &0 \le c_n \le 1, \quad c_n \in \mathbb{Z}, \quad \forall n \in V \\ &0 \le \hat{f}^1\big((i,j)\big) \le 1 \quad \forall (i,j) \in E \quad \Big\} \text{ time step 1} \\ &0 \le \hat{f}^2\big((i,j)\big) \le 1 \quad \forall (i,j) \in E \quad \Big\} \text{ time step 2} \end{aligned} \tag{8}$$

Power flow only on edges from surplus BSs to deficit BSs:

$$\begin{aligned} &\hat{f}^1\big((i,j)\big) + c_i \le 1 \quad \forall (i,j) \in E \\ &\hat{f}^1\big((i,j)\big) - c_j \le 0 \quad \forall (i,j) \in E \end{aligned} \Big\} \text{ time step 1}$$
$$\begin{aligned} &\hat{f}^2\big((i,j)\big) + c_j \le 1 \quad \forall (i,j) \in E \\ &\hat{f}^2\big((i,j)\big) - c_i \le 0 \quad \forall (i,j) \in E \end{aligned} \Big\} \text{ time step 2} \tag{9}$$

Power flow out of the surplus BSs:

$$\sum_{\substack{(i,j)\in E \\ j\in V}} \hat{f}^1\big((i,j)\big) \le \hat{b}_0 \quad \forall i \in V \Big\} \text{ time step 1}$$
$$\sum_{\substack{(i,j)\in E \\ j\in V}} \hat{f}^2\big((i,j)\big) \le \hat{b}_0 \quad \forall i \in V \Big\} \text{ time step 2} \tag{10}$$

Power flow into the deficit BSs:

$$\underbrace{\sum_{\substack{(i,j)\in E \\ i\in V}} \hat{f}^1\big((i,j)\big)\big(1 - C \cdot d\big((i,j)\big)\big) \le |\hat{b}_1| \quad \forall j \in V}_{\text{time step 1}}$$
$$\underbrace{\sum_{\substack{(i,j)\in E \\ i\in V}} \hat{f}^2\big((i,j)\big)\big(1 - C \cdot d\big((i,j)\big)\big) \le |\hat{b}_1| \quad \forall j \in V}_{\text{time step 2}} \tag{11}$$

The optimization objective (7) adds the normalized power flows on all edges and subtracts the normalized power losses (cf. (3)) on all edges.

The inequalities (8) represent the lower bounds and the upper bounds for the parameters to be determined, i.e., for the parameters c_n, $\hat{f}^1\big((i,j)\big)$ and $\hat{f}^2\big((i,j)\big)$ for all $n \in V$ and $(i,j) \in E$. In addition, the inequalities (8) state that the parameters c_n are integers for all $n \in V$.

The inequalities (9) ensure that power only flows on edges from surplus BSs to deficit BSs. Power can only flow on an edge (i,j) in time step 1 if BS_i belongs to cluster 0, i.e., $c_i = 0$, and BS_j belongs to cluster 1, i.e., $c_j = 1$. $\hat{f}^1\big((i,j)\big) + c_i \le 1$ implies that the power flow $\hat{f}^1\big((i,j)\big)$ is 0 if c_i is not 0 and $\hat{f}^1\big((i,j)\big) - c_j \le 0$ implies that the power flow $\hat{f}^1\big((i,j)\big)$ is 0 if c_j is not 1 in time step 1. Vice versa in time step 2, power can only flow on an edge (i,j) if BS_i belongs to cluster 1, i.e., $c_i = 1$, and BS_j belongs to cluster 0, i.e., $c_j = 0$. $\hat{f}^2\big((i,j)\big) + c_j \le 1$ implies that the power flow $\hat{f}^2\big((i,j)\big)$ is 0 if c_j is not 0 and $\hat{f}^2\big((i,j)\big) - c_i \le 0$ implies that the power flow $\hat{f}^2\big((i,j)\big)$ is 0 if c_i is not 1 in time step 2.

The inequalities (10) ensure that the normalized power flow out of a surplus BS is not greater than $\hat{b}_0$. If $i \in V$ is a deficit BS in time step t, then $\sum_{\substack{(i,j)\in E \\ j\in V}} \hat{f}^t\big((i,j)\big) \le \hat{b}_0$ is already fulfilled because all power flows out of the deficit BS_i are 0 due to the inequalities (9).

The inequalities (11) ensure that the normalized power flow into a deficit BS is not greater than $|\hat{b}_1|$. The power received at the deficit BSs is subject to power losses in the transmission lines. If $j \in V$ is a surplus BS in time step t, then $\sum_{\substack{(i,j)\in E \\ i\in V}} \hat{f}^t\big((i,j)\big)\big(1 - C \cdot d\big((i,j)\big)\big) \le |\hat{b}_1|$ is already fulfilled because all power flows into the surplus BS_j are 0 due to the inequalities (9).

VI. Numerical Results

We use the intlinprog(f, intcon, A, b) function implemented in MATLAB to solve the mixed-integer linear programming problem (MILPP) defined in (7)-(11). Unless otherwise stated, we use the values[2] from Table I for the parameters to evaluate the performance of our proposed MILPP.

We generate 1000 random graphs to determine the average normalized renewable power M received at the deficit BSs during the two time steps (cf. (7)). The random graphs are generated by placing the N BSs uniformly in the square and connecting any two BSs with a probability of $q \in [0,1]$ with a transmission line.

TABLE I: Input parameters

Parameter	Value
$C \in [0, \frac{1}{\sqrt{2}}]$	0.6
$N \in \mathbb{N}$	8
$q \in [0,1]$	0.3
$b_0 \in \mathbb{R}^+$	1
$b_1 \in \mathbb{R}^-$	-1

We investigate the performance of our proposed MILPP in comparison with randomly allocating BSs into clusters, i.e., without considering the topology of the cellular network

[2]Without loss of generality, we set $b_0 = 1$ and $b_1 = -1$, because the energy harvesting device types should have similar capacities and all power values will be normalized in (6) anyway.

or the power losses in the transmission lines by setting the cluster allocation values c_i at 0, and 1 with a probability of 50%, and 50%, respectively. In other words, $\mathbb{P}(c_i = 0) = \mathbb{P}(c_i = 1) = 0.5 \ \forall i$ for the random cluster allocation.

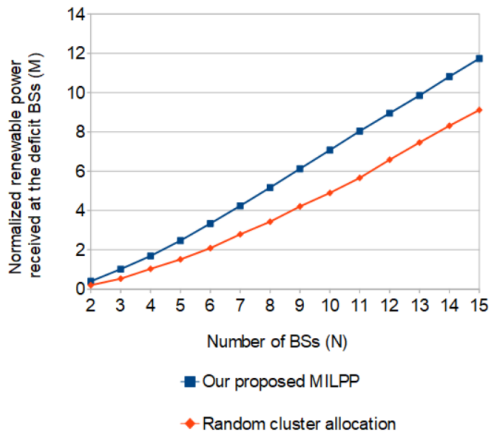

Fig. 5: Average normalized renewable power received at the deficit BSs (M) of our proposed MILPP and of random BS cluster allocation vs. number of BSs (N).

Fig. 5 shows the performance of our proposed MILPP and of random BS cluster allocation for different numbers of BSs (N). The performance gap between the two BS cluster allocations increases with the number of BSs. This is because a denser cellular network offers more opportunities for BS clustering optimization, and hence the superiority of the MILPP over the random BS cluster allocation increases with the cellular network density.

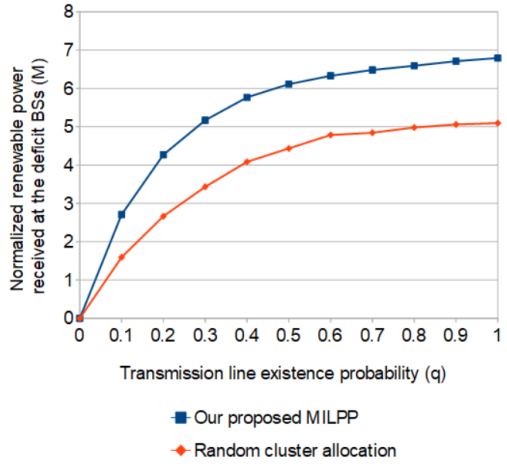

Fig. 6: Average normalized renewable power received at the deficit BSs (M) of our proposed MILPP and of random BS cluster allocation vs. transmission line existence probability (q).

Fig. 6 shows the performance of our proposed MILPP and of random BS cluster allocation for different transmission line existence probabilities (q). The performance gap between the two BS cluster allocations increases with the transmission line existence probability in the range of 0 to 0.3 whereas it is nearly constant in the range of 0.3 to 1.

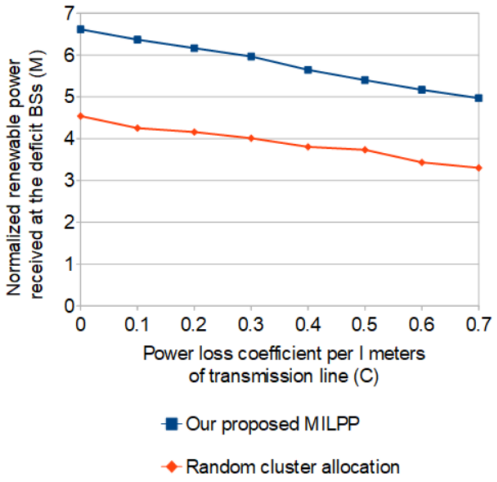

Fig. 7: Average normalized renewable power received at the deficit BSs (M) of our proposed MILPP and of random BS cluster allocation vs. power loss coefficient per l meters of transmission line (C).

Fig. 7 shows the performance of our proposed MILPP and of random BS cluster allocation for different power loss coefficients per l meters of transmission line (C)[3]. The performance gap between the two BS cluster allocations decreases slightly with the power loss coefficient per l meters of transmission line.

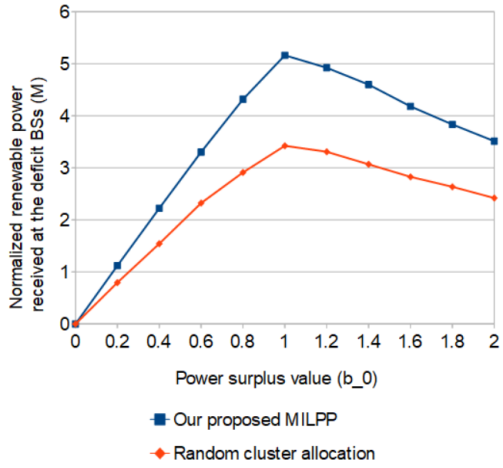

Fig. 8: Average normalized renewable power received at the deficit BSs (M) of our proposed MILPP and of random BS cluster allocation vs. power surplus value (b_0). b_1 was fixed to -1.

Fig. 8 shows the performance of our proposed MILPP and of random BS cluster allocation for different power surplus values (b_0). b_1 was fixed to -1. The performance gap between the two BS cluster allocations increases with the power surplus value in the range of 0 to 1 whereas it decreases in the range of 1 to 2. This is because the power was normalized with respect to $\max\{b_0, |b_1|\}$. If $b_0 \neq 1$, either $\hat{b}_0$ or $|\hat{b}_1|$ is smaller than 1 because a mismatch exists between the power surplus

[3]We use the normalized Euclidean distance $d\big((i,j)\big) = \frac{||BS_i - BS_j||}{l}$ in all formulas, derived parameters and the proposed MILPP. Hence, the results in Fig. 7 do not change with different values of l, only the scale of the x-axis changes. If the BSs are deployed in an area of, e.g., 1000 m x 1000 m, Fig. 7 should be read with the x-axis label "Power loss coefficient per 1000 meters."

value and the power deficit value. Only if $b_0 = 1$, $\hat{b}_0$ and $|\hat{b}_1|$ are both 1 because the power surplus value and the power deficit value have the same absolute value.

Figs. 5 - 8 show that our proposed MILPP always outperforms the random BS cluster allocation because the MILPP considers the topology of the cellular network and the power losses in the transmission lines. Because our proposed MILPP takes into account the topology of the cellular network, it increases the probability that a BS is deployed with an energy harvester type that is anti-correlated to those deployed at its connected neighboring BSs. In addition, the shorter the transmission line between a pair of BSs, the more likely that these two BSs are deployed with anti-correlated energy harvesters, because our proposed MILPP takes into account the distance-dependent power loss in the transmission lines.

VII. Conclusion

We have developed an optimization algorithm to determine how energy harvesters with anti-correlated energy generation profiles should be deployed to every BSs to use the renewable power more efficiently. If energy harvesters with anti-correlated energy generation profiles are deployed at BSs that are connected by transmission lines, the power can be transmitted from surplus BSs to deficit BSs via the transmission lines. The proposed optimization algorithm is based on a mixed-integer linear programming problem and can be run once during the cellular network planning. There are two different types of energy harvesters, which have anti-correlated energy generation profiles, available for deployment in our system model. By taking into account the topology of the cellular network, i.e., whether or not a transmission line exists between a pair of BSs, our proposed algorithm increases the probability that a BS is deployed with an energy harvester type that is anti-correlated to those deployed at its connected neighboring BSs. In addition, the shorter the transmission line between a pair of BSs, the more likely that these two BSs are deployed with anti-correlated energy harvesters, because our proposed algorithm takes into account the distance-dependent power loss in the transmission lines. The renewable power that can be transmitted from the surplus BSs to the deficit BSs in the cellular network is on average around 40% higher with our proposed optimization algorithm in comparison with randomly deploying anti-correlated energy harvesters to the BSs.

Acknowledgment

This work was supported by the A*STAR-Sheffield Research Attachment Programme. This work was partly funded by the European Unions Horizon 2020 Research and Innovation Programme under grant agreement No 645705 and by the A*STAR Industrial Internet of Things Research Program, under the RIE2020 IAF-PP Grant A1788a0023.

References

[1] M. D. Mueck, I. Karls, R. Arefi, T. Haustein, R. J. Weiler, and K. Sakaguchi, "Global standards enabling a 5^{th} generation communications system architecture vision," in *Proc. IEEE GLOBECOM Workshops*, Dec 2014, pp. 571–576.

[2] Y. Mao, Y. Luo, J. Zhang, and K. B. Letaief, "Energy harvesting small cell networks: feasibility, deployment, and operation," *IEEE Communications Magazine*, vol. 53, no. 6, pp. 94–101, Jun 2015.

[3] A. Kwasinski and A. Kwasinski, "Increasing sustainability and resiliency of cellular network infrastructure by harvesting renewable energy," *IEEE Communications Magazine*, vol. 53, no. 4, pp. 110–116, Apr 2015.

[4] Y. K. Chia, S. Sun, and R. Zhang, "Energy cooperation in cellular networks with renewable powered base stations," *IEEE Transactions on Wireless Communications*, vol. 13, no. 12, pp. 6996–7010, Dec 2014.

[5] J. N. V. Lucas, G. E. Francés, and E. S. M. González, "Energy security and renewable energy deployment in the EU: Liaisons dangereuses or virtuous circle?" *Renewable and Sustainable Energy Reviews*, vol. 62, pp. 1032–1046, Sep 2016.

[6] X. Li, "Diversification and localization of energy systems for sustainable development and energy security," *Energy Policy*, vol. 33, no. 17, pp. 2237–2243, Nov 2005.

[7] L. Cerović, D. Maradin, and S. Čegar, "From the restructuring of the power sector to diversification of renewable energy sources: Preconditions for efficient and sustainable electricity market," *International Journal of Energy Economics and Policy*, vol. 4, no. 4, pp. 599–609, 2014.

[8] D. Benda, X. Chu, S. Sun, T. Q. S. Quek, and A. Buckley, "Renewable energy sharing among base stations as a min-cost-max-flow optimization problem," *IEEE Transactions on Green Communications and Networking*, vol. 3, no. 1, pp. 67–78, March 2019.

[9] X. Huang and N. Ansari, "Energy sharing within EH-enabled wireless communication networks," *IEEE Wireless Communications*, vol. 22, no. 3, pp. 144–149, Jun 2015.

[10] D. Benda, X. Chu, S. Sun, T. Q. S. Quek, and A. Buckley, "Modeling and optimization of energy sharing among base stations as a minimum-cost-maximum-flow problem," in *Proc. IEEE VTC-Spring*, Porto, Portugal, Jun 2018.

[11] D. Benda, S. Sun, X. Chu, T. Q. S. Quek, and A. Buckley, "PV cell angle optimization for energy generation-consumption matching in a solar powered cellular network," *IEEE Transactions on Green Communications and Networking*, vol. 2, no. 1, pp. 40–48, March 2018.

[12] D. Benda, X. Chu, S. Sun, T. Q. S. Quek, and A. Buckley, "PV cell angle optimisation for energy arrival-consumption matching in a solar energy harvesting cellular network," in *Proc. IEEE ICC*, Paris, France, May 2017.

[13] D. Benda, X. Chu, S. Sun, T. Q. S. Quek, and A. Buckley, "PV cell orientation angle optimization for a solar energy harvesting base station," in *Proc. IEEE GLOBECOM*, Singapore, Dec 2017.

[14] European Commission. (2016) Photovoltaic geographical information system (pvgis). [Online]. Available: http://re.jrc.ec.europa.eu/pvgis/

[15] H. Cole and D. Sang, *Revise AS Physics for AQA A*. Oxford, United Kingdom: Heinemann Educational Publishers, 2001, pp. 67–68.